AIP Advances

Experimental and numerical study on capillary flow along deflectors in plate surface tension tanks in microgravity environment

Cite as: AIP Advances **9**, 025020 (2019); https://doi.org/10.1063/1.5083672
Submitted: 30 November 2018 . Accepted: 23 January 2019 . Published Online: 19 February 2019

Shangtong Chen, Zhiyi Han, Li Duan, and Qi Kang

ARTICLES YOU MAY BE INTERESTED IN

Experimental and numerical study on capillary flow along deflectors in plate surface tension tanks in microgravity environment

Cite as: AIP Advances 9, 025020 (2019); doi: 10.1063/1.5083672
Submitted: 30 November 2018 • Accepted: 23 January 2019 •
Published Online: 19 February 2019

Shangtong Chen,[1,2] Zhiyi Han,[1,2] Li Duan,[1,2] and Qi Kang[1,2,a)]

AFFILIATIONS

[1] Key Laboratory of Microgravity, Institute of Mechanics, Chinese Academy of Sciences, Beijing 100190, China
[2] College of Engineering & Science, University of Chinese Academy of Sciences, Beijing 100049, China

[a)] Corresponding author: kq@imech.ac.cn

ABSTRACT

Surface tension tanks are the most widely used satellite propellant tanks, which use liquid surface tension for liquid transportation and gas-liquid separation to provide pure propellant for thruster. As the second generation surface tension tank, the plate type tank has characteristics of simple structure, easy processing and high reliability, and represents development direction of surface tension tanks. In this paper, drop tower experiments are used to investigate transfer speed of deflectors in plate type tanks, and corresponding numerical simulation is carried out in Fluent with Volume of Fluid method.

I. INTRODUCTION

At 15:04:09 on September 15, 2016, Tiangong-2 Space Laboratory successfully launched by the ChangZheng-2F rocket at Jiuquan Satellite Launch Center. It is the second space laboratory independently developed by China after Tiangong-1. In this process, the propulsion system plays an important role.

In microgravity environment, gravity influence basically disappears, and secondary forces such as surface tension force play a dominant role, so liquid behavior in microgravity environment will be significantly different from that on the ground,[1] the tank for storing propellant is usually co-existing with gas and liquid, and precise control of liquid in coexistence of gas and liquid is the biggest challenge of tank design. The main problems of fluid management in space are static balance of liquid propellant, repositioning,[2] liquid sloshing, capillary flow and gas-liquid separation.[3,4] Among them, liquid transportation speed of the deflector determines the time required for static balance after getting into microgravity environment and liquid repositioning during orbit control. The capillary flow along deflectors and separation of gas and liquid are main concerns for providing pure propellant for propulsion system. Therefore, it is important to properly design structure of deflectors.

Countries advanced in aerospace engineering such as the United States and Russia attach great importance to in-orbit fluid management technology. They have carried out a number of space and ground verification experiments, and have achieved remarkable results and accumulated rich experience.

In 1975, the National Aeronautics and Space Administration (NASA) launched Viking Satellite for pirate program.[5] Pirates 75 satellite's tank is the first plate surface tension tank for flight in the world. The main structure of its propellant management device (PMD) is a component consisting of some deflectors and a liquid accumulator.

In 1987, Hughes Space Communications Corporation (HSC) introduced HS601,[6] the company's most successful geostationary orbit satellite platform. The PMD of its tank is mainly composed of plate structure, including four orthogonally placed deflectors, an accumulator, a bubble trap, a tubular collector and a capillary net window. The tank is of the type that transits from screen type to plate type. In 1996, HSC optimized HS601HP, the structure of which is very similar to that of HS601. According to the flow need, a 1.18-meter-long cylindrical section is added to the HS601, and length of the deflector is also increased correspondingly.

FARE2 project[7] was hosted by Lockheed Martin Space Center in June 1993. Its main purpose is to study on-orbit extrusion performance of the new generation of plate surface tension tank and positioning and static characteristics of liquid in the plate surface tension tank.

Besides space projects mentioned above, many scholars have conducted plenty of researches about design of PMD from theory, numerical simulation and experiments, and obtained many important results.

In theoretical research aspect, many researchers have analyzed static liquid surface shapes in various containers as early as the 1960s. Concus and Finn et al.[8,9] studied liquid equilibrium interface in vessels with internal angles and proposed the famous Concus-Finn condition.[10] If θ is the contact angle, α is half of the internal angle, in no gravity condition, when $\theta+\alpha > 90°$, there is a stable equilibrium interface at inner corner of container, that is, liquid will have a stable interface configuration at the inner corner. When $\theta+\alpha < 90°$ (Concus-Finn condition), liquid interface at the inner corner cannot stably exist, that is, liquid will continuously climb along the inner corner. In 1996, Weislogel et al.[11] considered influence of liquid inertial force, and carried out theoretical analysis combined with short-time microgravity drop tower experiments to study capillary flow of rectangular section container satisfying the Concus-Finn condition, and established Navier-Stokes equation of capillary flow at the inner corner. Infinitely long capillary flow is solved by the perturbation method. Numerical results of capillary flow in viscous phase is basically consistent with experimental results. In China, Wei Yuexing, Chen Xiaoqian et al.[12] studied equation of capillary flow at the inner corner. By correcting calculation of radius of curvature, relationship between section and radius of curvature was found, so that it can be applied to different contact angles and different dihedral angles. The problem of the least squares finite element method is corrected, the quadratic solution of the inner angular flow is obtained, and the capillary flow principle is applied to the design of the tank.

In numerical simulation and microgravity experiments aspects, in 1991, DE Jaekle[13] analyzed transportation mechanism of deflectors, accumulators, traps, grooves and corridors of PMD under microgravity environment, laying the foundation of design and analysis of the second surface tension tank. At the same time, the two-step LAX-Wendroff numerical solution method is used to discretize control equations and calculate driving ability of deflectors. Propellant transportation process of deflectors in unsteady state of engine ignition and extinction is simulated. And the time from engine ignition to propellant stable transportation is obtained, which provides calculation basis for design of plate tanks. In 2002, SH Collicott[14] used Surface Evolver to carry out three-dimensional numerical simulation of liquid flow in the plate tank in VTRE project under microgravity environment, and obtained three-dimensional interface distribution during fluid transportation, which verified Surface Evolver's correctness as an accurate means of designing PMD. In China, Li Yong, Pan Hailin and others[15] studied propellant's behavior in plate tanks, and simulated constant flow and unsteady flow respectively. Wang Yi et al.[16] carried out numerical simulation of balance interface of propellant in plate tanks and analyzed in detail. Zhang Chenhui et al.[17] used Surface Evolver to conduct preliminary simulation about three-dimensional gas-liquid equilibrium interface in tanks, and promoted applicability of Concus-Finn theory at inner corner. Wei Yanming et al.[18] conducted a drop tower experiment using reduction ratio model of fully managed cylindrical surface tension tank and studied repositioning process of propellant, verifying on-orbit performance of the surface tension tank. Zhuang Baotang et al[19] carried out the drop tower experiments about transportation velocity of deflectors in the microgravity environment. The deflectors with different cross section shapes have a great influence on fluid transportation speed. Reasonable design of cross-sectional shape of deflectors can effectively control transportation speed and provide pure propellant for propellers.

II. MICROGRAVITY EXPERIMENTS

A. Experimental preparation

Drop tower tests can provide short microgravity environment, but relatively low gravitational acceleration. It is the most commonly used microgravity experimental method.

This study chooses the single cabin type. During experiments, the cabin is free to fall in atmospheric environment and reaches microgravity level of 10^{-3}g. Its microgravity environment can last for 3.5s.

According to research requirements of single cabin experiments, an experimental platform is established. The experimental platform consists of tank models, model holders, a lighting device, an image acquisition device, a microgravity indication system, etc. Its diameter is 800 mm and the platform is shown in Fig. 1.

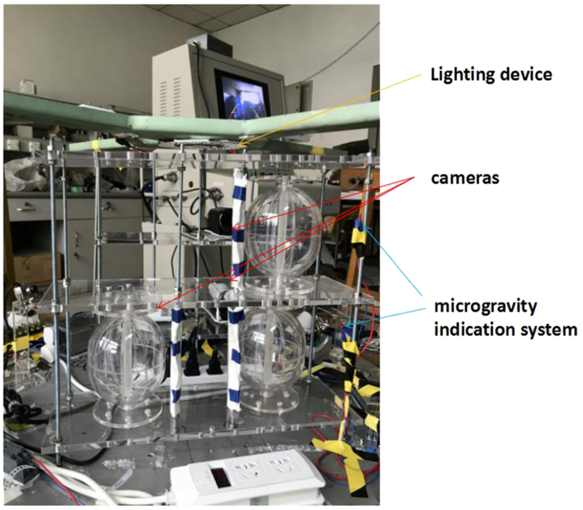

FIG. 1. Experimental Platform.

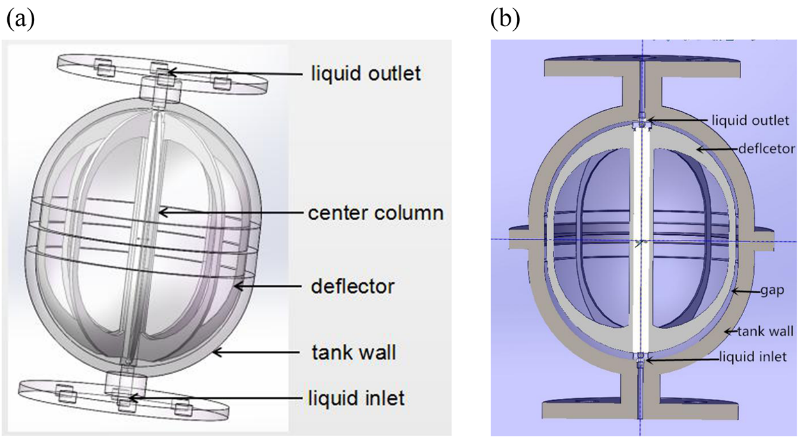

FIG. 2. (a) A tank model and (b) section of a tank model.

The tank model is made of transparent polymethyl methacrylate (PMMA), as shown in Fig. 2 The total height of the model is 161mm and its inner diameter is 109mm.The tank wall is composed of two hemispheres and one cylindrical section, and its PMD is an assembly which contains 8 identical deflectors. There are certain gaps between deflectors and tank wall. At the cylindrical section, the gaps of the three tanks are 0.5mm wide, 1.0mm wide and 1.5mm wide respectively. In order to make full use of capillary driven force, the gaps become smaller and smaller from liquid inlet to liquid outlet, and the variation intervals are 0.6-0.4mm, 1.1-0.9mm, 1.6-1.4mm. (Hereinafter, for convenience of description, the three different-size gaps are considered to be 0.5 mm, 1.0 mm, and 1.5 mm wide respectively).

The experimental medium used was anhydrous ethanol stained with rhodamine, and its physical properties are shown in Table I. The contact angle of absolute ethanol with PMMA is 1°. The angle of the corner between deflector and tank wall is 90°. According to Concus-Finn theory,[10] when the contact angle that the liquid makes with the solid wall is smaller than 45 degree, spontaneous capillary flow (SCF) will occur. Therefore, there will be SCF when using anhydrous ethanol to do experiments. And the smaller the contact angle is, the better the spreadability of anhydrous ethanol on PMMA will be, which is beneficial to speed of SCF in tanks under microgravity environment.

A plurality of scale papers are attached to the outer wall of tanks for measuring liquid flow speed. In the same shooting range, liquid flow along 1-3 deflectors near scale papers can be observed. The position of liquid leading edge on each deflector at different times is recorded, and the average value is taken as climb distance and climb speed.

B. Experimental results

In this paper, I have done several experiments under two different conditions. One is that the tank models are placed in the forward direction with 25% filling rate, the other is that the tank models are placed in the opposite direction with 50% filling rate. Under forward placed condition, the liquid inlet of tanks is in the bottom and liquid gathers near the liquid inlet in the beginning. And under reversed placed condition, the liquid outlet is in the bottom and liquid gathers near the liquid outlet in the beginning.

Fig. 3 and Fig. 4 show anhydrous alcohol interface at different times under two operation conditions. It can be seen clearly that absolute ethanol flows rapidly at the gap while flows slowly on the wall, forming a concave liquid surface on the wall. Record position of the leading edges of the liquid at different times in each experimental results and take their average. Tabulate the data and draw figures as shown in Fig. 5 and Fig. 6.

In the first case liquid flow speed in the tank with 1.0mm-wide gaps is the fastest, which reaches 58.5mm/s. And it's slightly faster than in the tank with 0.5mm-wide gaps. Liquid flow speed in tanks with 1.0mm-wide gaps and 0.5mm-wide gaps are significantly faster than in the tank with 1.5mm-wide gaps.

In the second case liquid flow speed in the tank with 1.0mm-wide gaps is slightly slower than in the tank with 0.5mm-wide gaps in the beginning and then becomes basically

TABLE I. Physical properties parameter of fluid (Ethanol solution with concentration 1/150000 Rhodamine B at 22°C).

Fluid	Density ρ(kg/m^3)	Surface tension coefficient σ(N/m)	Dynamic viscosity μ(Pa·s)	Contact angle θ (°)
anhydrous ethanol	789	0.0213	0.00117	1

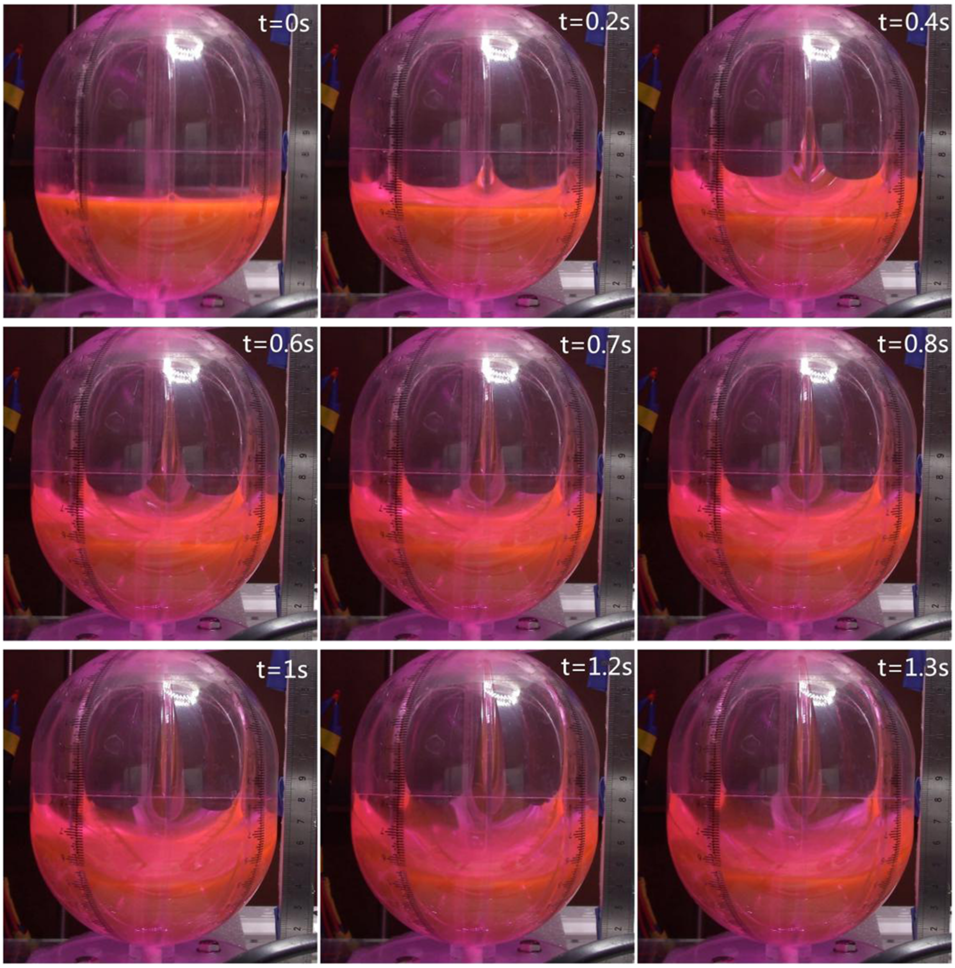

FIG. 3. Anhydrous alcohol interface at different times during drop tower tests in the tank with 1.0mm-wide gaps. The tank is forward placed with 25% filling ratio.

equal. Liquid flow speed in tanks with 1.0mm-wide gaps and 0.5mm-wide gaps is significantly faster than in the tank with 1.5mm-wide gaps.

III. NUMERICAL SIMULATION

A. Introduction of mathematical model

To further study fluid behavior in tanks, use ICEM to establish mathematical model and Fluent with VOF method to do corresponding simulation. Volume of Fluid (VOF) method[20] can deal with strong nonlinear phenomena such as large deformation of free surface effectively. The position and shape of free surface is determined by calculating ratio function F of volume of liquid in grid cell and volume of the grid cell itself.

In order to improve calculation speed, divide hexahedron structure grid with one-eighth of the tank model. Since the flow along deflectors is mainly considered, for the convenience of modeling, both liquid outlet and inlet are sealed. And both ends of the center column are simplified, for example, openings and steps are simplified into cylindrical segments, as shown in Fig. 7(a) and Fig. 7(b).

The mathematical model includes five parts: symmetry, tank wall, center column, deflectors and internal fluid domain, as Fig. 8 shows. Boundary layers are established near all solid walls, including tank wall, center column and deflectors. Its expansion ratio is 1.2 and the height of the first layer is smaller than 0.1mm.The total number of grids is about 1.1 million.

B. Parameter settings

Taking into account microgravity level of the single cabin drop tower experiments, gravitational acceleration g is set to be 0.005 m/s^2 during the simulation.

It is estimated from experimental results that the characteristic scale of liquid flow is 2mm, and the characteristic velocity of liquid flow is 0.06m/s. According to *Re* number equation,

$$\mathrm{Re} = \frac{\rho v l}{\mu} \tag{1}$$

Re number of liquid flow in the tanks can be calculated to be about 81. For internal flow, when $Re<2000$, the flow mode is laminar flow, therefore we choose the laminar flow as flow mode during simulation.

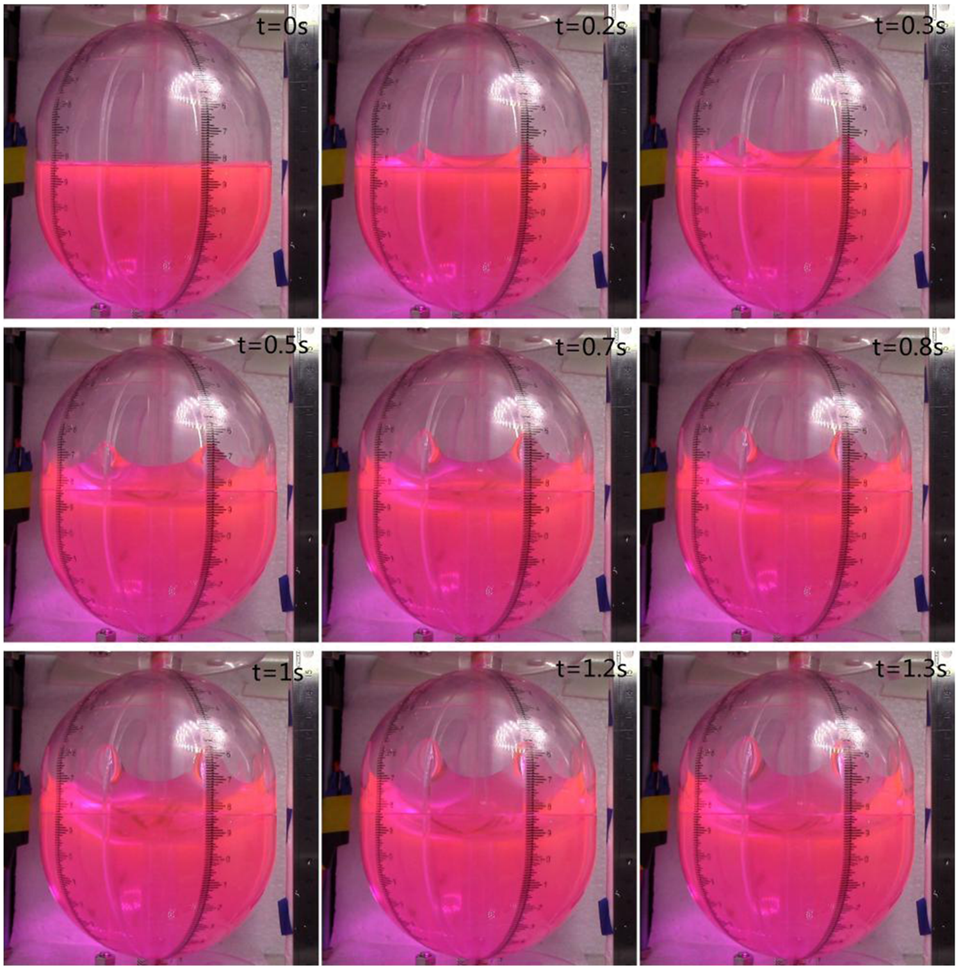

FIG. 4. Anhydrous alcohol interface at different times during drop tower tests in the tank with 1.5mm-wide gaps. The tank is reversed placed with 50% filling ratio.

The pressure-velocity coupling equation is numerically solved by SIMPLEC algorithm. The SIMPLEC algorithm uses a relationship between velocity and pressure corrections to enforce mass conservation and to obtain the pressure field.

Time step size is 0.0001s and do 30 iterative calculation per time step. The gradient spatial discretization equation is based on Least Square Cell. PRESTO is used for pressure spatial discretization equation. The momentum spatial discretization equation uses second-order upwind style, and Geo-Reconstruct is used for volume fraction spatial discretization equation. When the equation iterative residual decreases to 10^{-6}, the calculation is considered to converge. The relaxation factor for each equation is set by default.

During calculation the Courant number is mostly smaller than 0.5, which indicates that the calculation process is relatively stable. The Courant number is of fundamental importance for transient flows. For a one-dimensional grid, it is defined by:

$$Courant = \frac{u\Delta t}{\Delta x} \tag{2}$$

Where u is the fluid speed, Δt is the timestep and Δx is the mesh size.

C. Analysis of results

This paper conducts numerical simulations under four different operating conditions to monitor liquid repositioning process in drop tower experiments, as shown in Table II.

As shown in Fig. 9(a) and 9(b), the left half part of the two images is experimental result, and the right half part is simulation result. The yellow surface in the right half part represents gas-liquid interface. It can be seen that in the two comparison images, the interface configuration of the experimental results is quite similar to that of numerical simulation results, including the position of the liquid leading edge at the gap and the shape of the concave liquid surface on the wall, etc., indicating that the simulation results are comparatively accurate.

As Fig. 10 presents, the red part represents liquid phase, and the blue part represents gas phase. It can be seen that flow speed of absolute ethanol at the gap is significantly faster than at other places.

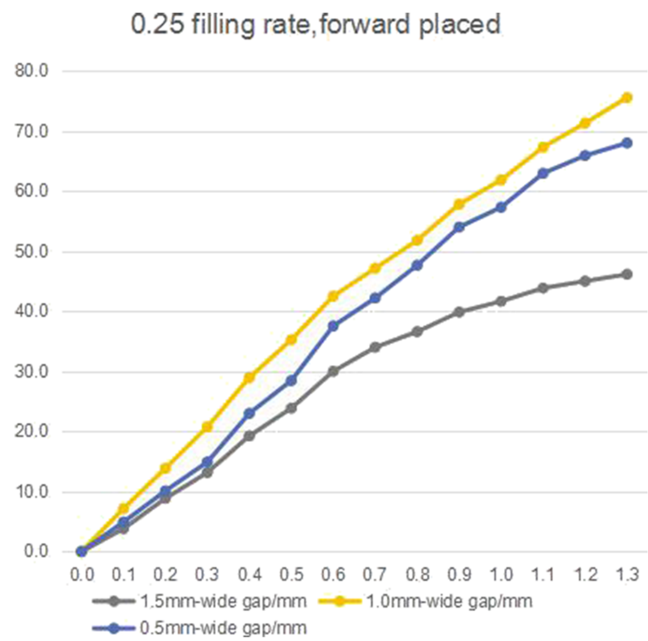

FIG. 5. Relationship between liquid flow distance and time in different tanks when tanks are forward placed with 25% filling ratio.

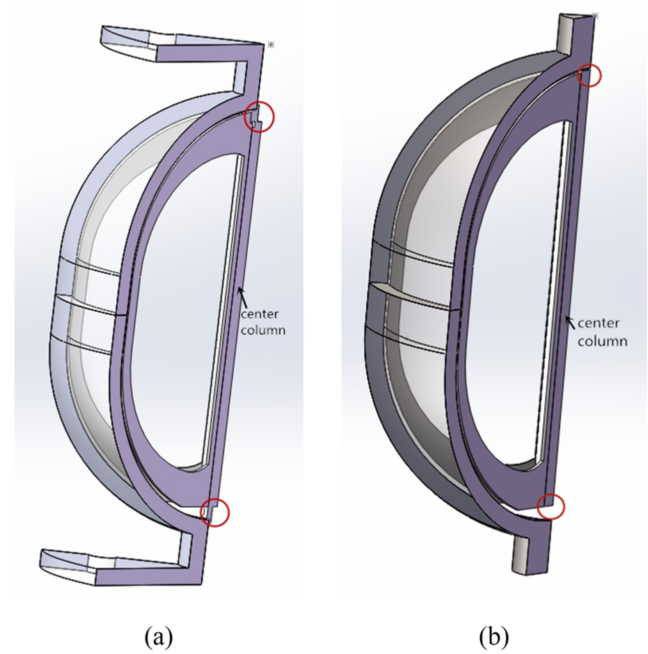

FIG. 7. (a) One-eighth of the tank model and (b) one-eighth of simplified tank model. As pointed by red circles, both ends of center column are simplified.

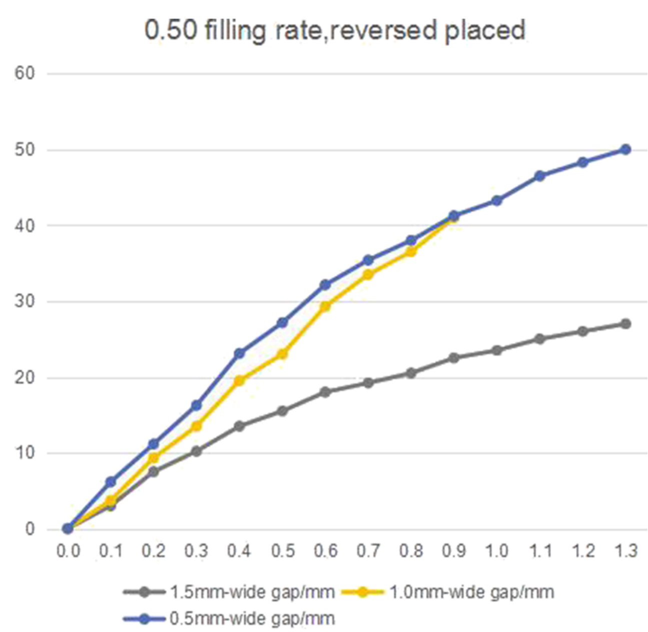

FIG. 6. Relationship between liquid flow distance and time in different tanks when tanks are reversed placed with 50% filling ratio.

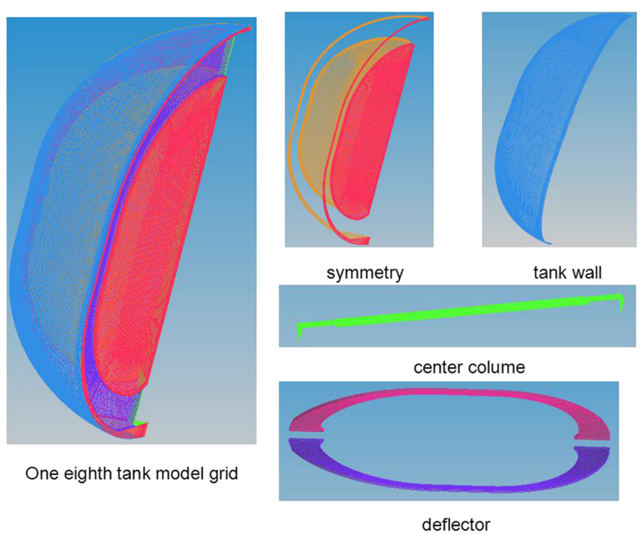

FIG. 8. Computational grid model.

TABLE II. different operating condition in the simulation.

placed direction / filling rate	forward placed	reversed placed
0.25	1	1
0.50	1	1

As shown in Fig. 11, the yellow surface represents gas-liquid interface. It can be seen that absolute ethanol still flows rapidly at the gap, and the flow velocity at other places is obviously slower, which forms a concave surface. Since the

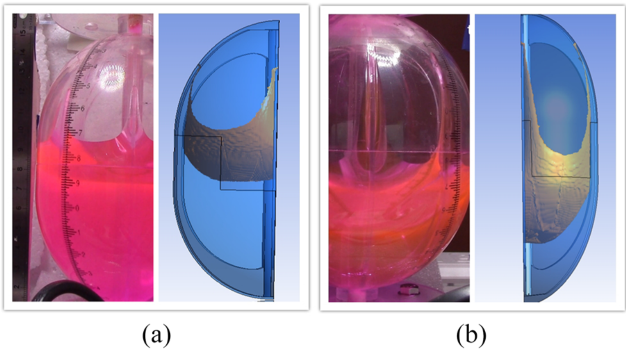

FIG. 9. Comparison of gas-liquid interface in drop tower tests and numerical simulation. (a) Gas-liquid interface in the tank with 0.5mm-wide gaps at t=0.5s. The tank is reversed placed with 50% filling ratio. (b) Gas-liquid interface in the tank with 1.0mm-wide gaps at t=1s. The tank is forward placed with 25% filling ratio.

liquid flow distance along deflectors cannot be directly measured in simulation results, the liquid flow velocity is indirectly reflected by change of liquid leading edge position in Y direction.

The liquid leading edge position in Y direction is determined as shown in Fig. 12. The contact point position between the gap and tank wall in the liquid leading edge is selected to

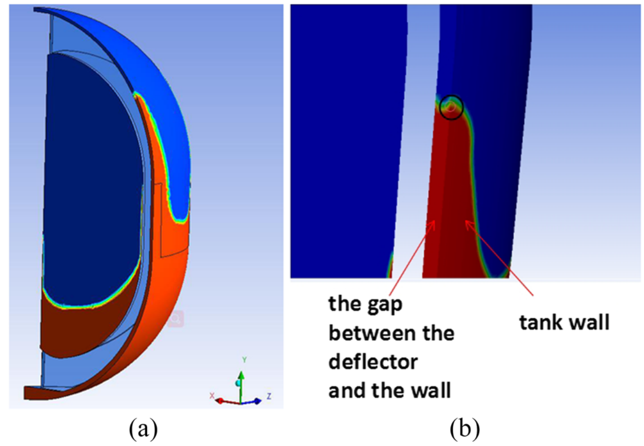

FIG. 12. (a) Liquid phase distribution and (b) the position pointed out by the black circle is the one chosen to measure the liquid leading edge position in *Y* direction.

measure the liquid leading edge position in Y direction. Results are shown in Figs. 13–16.

Because tank wall is composed of two hemispheres and one cylindrical section, value of liquid flow distance is larger than value of liquid leading edge position's change in Y

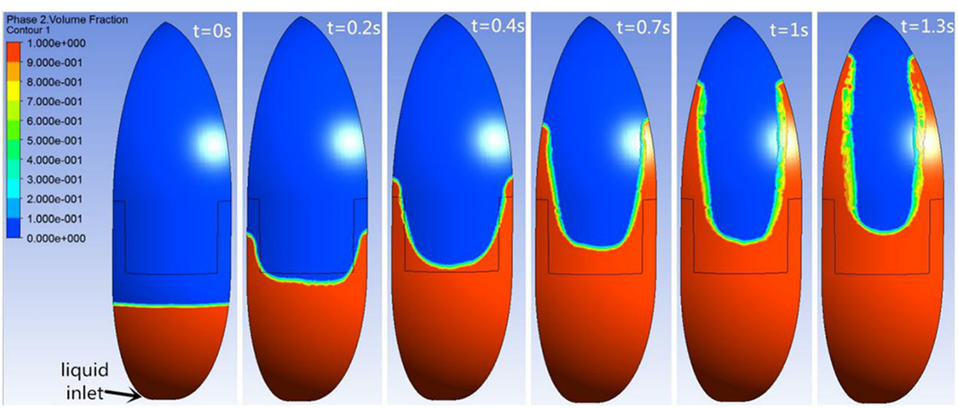

FIG. 10. Liquid phase distribution at different times on the tank wall. The tank is forward placed with 25% filling ratio, and width of the gaps between deflectors and tank wall is 1.0mm.

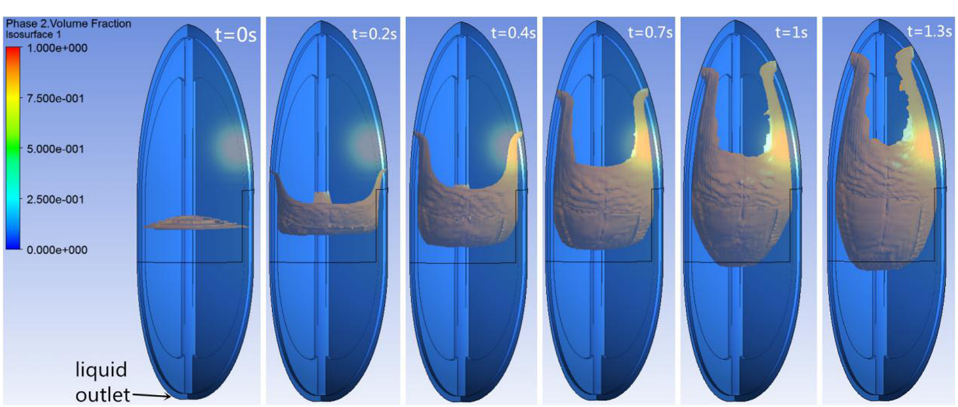

FIG. 11. Gas-liquid interface at different times in a tank. The tank is reversed placed with 50% filling ratio, and width of the gaps between deflectors and tank wall is 1.5mm.

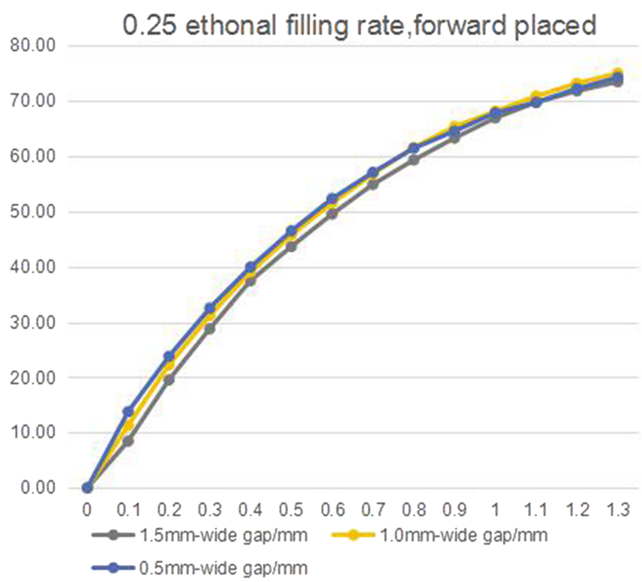

FIG. 13. Relationship between change of the liquid leading edge position in *Y* direction and time. The tanks are forward placed with 25% filling ratio.

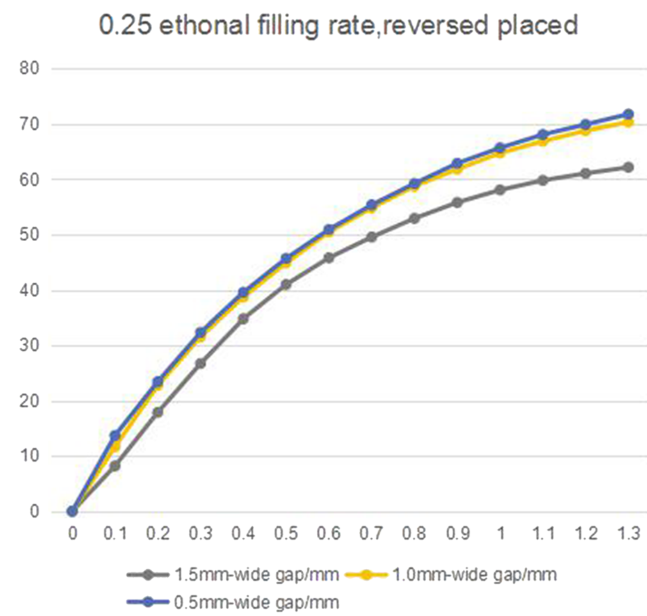

FIG. 15. Relationship between change of the liquid leading edge position in *Y* direction and time. The tanks are reversed placed with 25% filling ratio.

direction. The closer the liquid leading edge is to the liquid outlet or inlet, the greater the difference will be. Therefore, the relationship between change of the liquid leading edge position in Y direction and time is nonlinear, which is different from the relationship between liquid flow distance and time in drop tower tests.

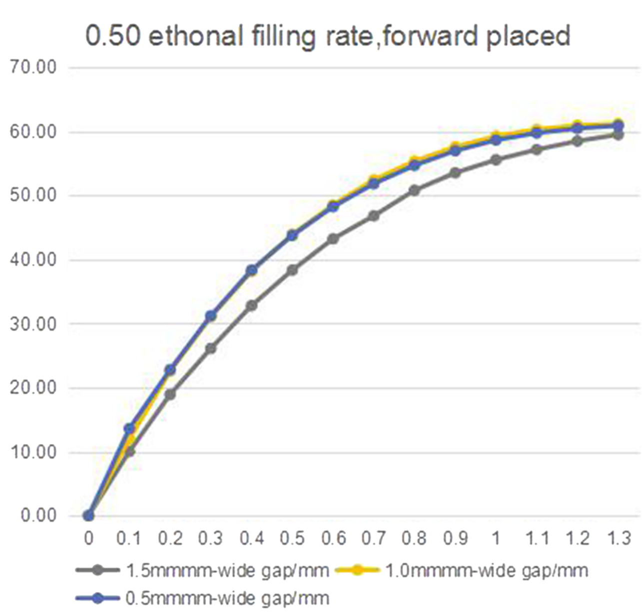

FIG. 14. Relationship between change of the liquid leading edge position in *Y* direction and time. The tanks are forward placed with 50% filling ratio.

As can be seen from Fig. 13–16, change of the liquid leading edge position in Y direction in tanks with 0.5mm-wide gaps and 1.0mm-wide gaps are very close, at the same time, they

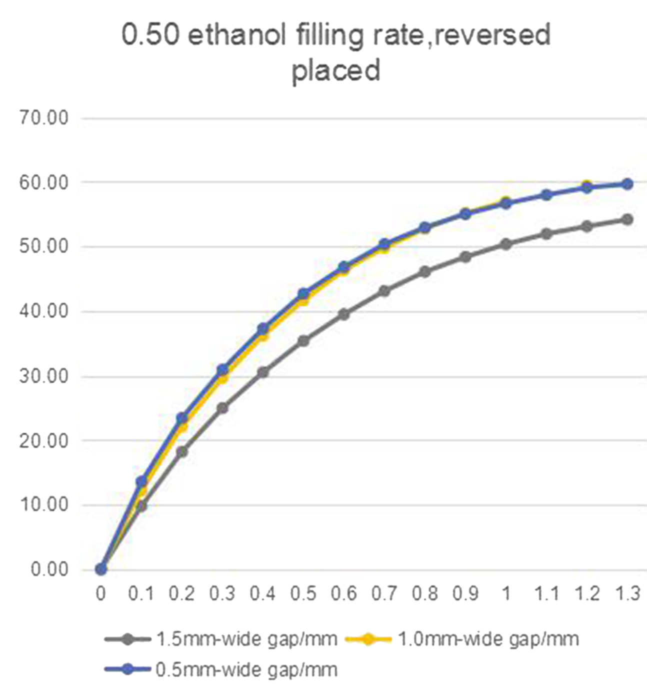

FIG. 16. Relationship between change of the liquid leading edge position in *Y* direction and time. The tanks are reversed placed with 50% filling ratio.

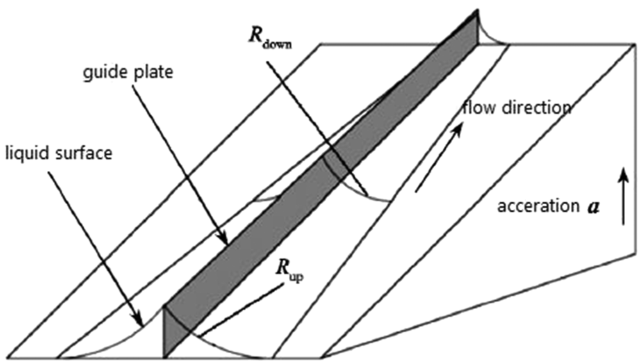

FIG. 17. Schematic diagram of capillary driven flow.

are also significantly faster than in the tank with 1.5mm-wide gaps.

As Fig. 13 shows, when tanks are forward placed with 25% filling ratio, liquid flow velocity in the tank with 1.0mm-wide gaps is slightly slower at first and then slightly faster than in tanks with 0.5mm-wide gaps, which is close to the experimental result.

As Fig. 16 shows, when tanks are reversed placed with 50% filling ratio, liquid flow velocity in the tank with 1.0mm-wide gaps is slower than in the tank with 0.5mm-wide gaps in the beginning, and then slightly faster, which is very close to the experimental result.

Fig. 17 is the schematic diagram of capillary driven flow in a plate tank under microgravity environment. Under the action of surface tension, a liquid belt with curvature is formed at the intersection of the deflector and tank wall. The Laplace formula is:

$$\Delta p = \sigma\left(\frac{1}{R_1} + \frac{1}{R_2}\right) \tag{3}$$

Where $R1$ and $R2$ are principal radius of curvature of the liquid belt, and for a certain section, it can be regarded as a cylindrical surface, therefore $R2=\infty$. Then pressure gradient due to difference in radius of curvature of the liquid belt, that is, the capillary driving force is:

$$\Delta p_{drive} = p_{up} - p_{down} = \sigma\left(\frac{1}{R_{down}} - \frac{1}{R_{up}}\right) \tag{4}$$

In normal gravity environment, capillary driven pressure equals static pressure, but when gravity disappears, the capillary driven pressure will drive liquid to climb along the internal angle or gap between deflectors and tank wall, which is called capillary driven flow. In Fig. 17, liquid flows along direction of the arrow and reaches a new equilibrium state.

Take one simulation result for example, as shown in Fig. 18(a) and 18(b), two liquid belt are formed along two deflectors. The radius of curvature of liquid belt in section I is smaller than in section II, which cause pressure gradient along flow direction that drives liquid flow along deflectors.

Furthermore, due to different width of gaps between deflectors and tank wall, liquid belts with different radius of curvature will form along deflectors, and the pressure gradient of a liquid belt in different tanks will be different, and that is the reason why liquid flow speed along deflectors in different tanks is different.

IV. CONCLUSIONS

With the development of space exploration, the need of reliable and efficient PMD increases rapidly. In the past few decades, many researches have been conducted to design PMD. This paper presents a new kind of PMD and conducts drop tower experiments and corresponding numerical simulation to investigate its transportation velocity.

Compared liquid flow speed at the gaps and tank wall, it can be seen that this kind of deflectors could ensure faster transportation speed, which can reduce propellant reorientation time when getting into microgravity environment remarkably. And liquid flow speed along defectors is not monotonously changed when value of gaps' width is between 0.5mm and 1.5mm. When gaps' width is 1.0mm, it is the most reasonable, whose transportation speed can reach 58.5mm/s.

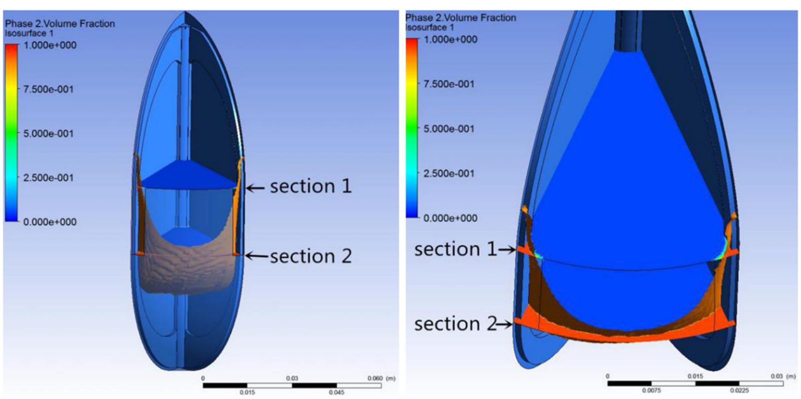

FIG. 18. (a) Gas-liquid interface in a simulation result and two sections which shows liquid phase distribution are established to observe liquid belt curvature and (b) see the result from another perspective.

ACKNOWLEDGMENTS

This research was funded by the China Manned Space Engineering program (Fluid Physics Experimental Rack, and TG-2 Liquid Bridge), and the National Natural Science Foundation of China (U1738116).

REFERENCES

[1] P. Concus and R. Finn, "On the behavior of a capillary surface in a wedge," Applied Mathematical Sciences **63**(2), 292–299 (1969).
[2] M. M. Weislogel, M. A. Sala, and S. H. Collicott, "Analysis of tank PMD rewetting following thrust resettling," In 40th AIAA Aerospace Sciences Meeting &Exhibit, Reno, January 2002.
[3] J. Faddoul and S. McIntype, "The NASA cryogenic fluid management facility program," AIAA/NASA/OAI Conference on Advanced SEI Technologies, Cleveland, September 1991.
[4] L. J. Hastings, S. P. Tucker, and C. F. Huffaker, "CFM technology needs for future space transportation systems," In AIAA/NASA/OAI Conference on Advanced SEI Technologies, Cleveland, September 1991.
[5] W. H. Tam and J. R. Taylor, "Design and manufacture of a propellant tank assembly," In 33rd AIAA/SAE/ASME/ASEE Joint Propulsion Conference, Seattle, July 1997.
[6] W. H. Tam, D. E. Jaekle, Jr., and S. A. Farokhi, "Design and manufacture of the HS 601 block II propellant tank assembly," In 34rd AIAA Joint Propulsion Conference, Seattle, July 1998.
[7] S. Dominick and J. Tegart, "Orbital test results of a vaned liquid acquisition device," AIAA94-3027, 1994.
[8] P. Concus and R. Finn, "On capillary free surfaces in the absence of gravity," Acta Math **132**, 177–198 (1974).
[9] P. Concus and R. Finn, "On capillary free surfaces in a gravitational Field," Acta Math **132**, 207–223 (1974).
[10] P. Concus and R. Finn, "Equilibrium liquid free-surface configurations–Mathematical theory and space experiments," AIAA 96-2047, 1996.
[11] M. M. Weislogel and S. Lichter, "Capillary flow in an interior corner," Journal of Fluid Mechanics **373**(1), 349–378 (1998).
[12] Y. X. Wei, X. Q. Chen, and Y. Y. Huang, "Interior corner flow theory and its application to the satellite propellant management device design," Sci China Tech Sci **54**, 1849–1854 (2011).
[13] D. E. Jaekel, Propellant management device conceptual design and analysis: Vanes, In 27th AIAA/SAE/ASME/ASEE Joint Propulsion Conference, Sacramento, July 1991.
[14] S. H. Collicott and M. M. Weislogel, "Modeling of the operation of the VTRE propellant management device, In 38th AIAA/SAE/ASME/ASEE Joint Propulsion Conference, Indianapolis, July 2002.
[15] Y. Li, H. Pan, Y. Wei *et al.*, "Numerical study on propellant flow in plate tanks under microgravity environment," Control Engineering **5**, 26–33 (2006).
[16] Y. Wang and X. Chang, "Numerical simulation of three dimensional gas-liquid equilibrium interfaces in the propellant tank under microgravity condition," Journal of Rocket Propulsion **33**(3), 31–35 (2007).
[17] C. Zhang, *Research on the Liquid Management in the Plate Surface Tension Tank under Microgravity* (Northeastern University, Shenyang, 2013).
[18] Y. Wei and H. Pan, "Microgravity experiment verification of fully managed cylindrical surface tension tank–Static balance and relocation," Control Engineering **5**(1), 14–19 (1997).
[19] B. Zhuang, Y. Li, H. Pan *et al.*, "Experiment investigation on transportation velocity of the fluid on propellant acquisition vanes under microgravity environment," Aerospace Control and Application **38**(6), 1–5 (2012).
[20] C. W. Hirt and B. D. Nichols, "Volume of fluid (VOF) method for the dynamics of free boundaries," Journal of Computational Physics **39**(1), 201–225 (1981).